Anomalous Diffusion in Strongly Coupled Quasi-2D Dusty Plasmas

Wen-Tau Juan and Lin I

Department of Physics and Center for Complex Systems, National Central University, Chung-Li, Taiwan 32054, Republic of China

(Received 7 April 1997)

The motions of dust particles in a strongly coupled quasi-2D dusty plasma system are studied using direct optical monitoring. After the short-time antipersistent caged stage, the series excitation and relaxation of rotational motions follow the random phase stick-slip rule for the harder melting state but are the non-stick-slip type for the softer liquid state. The former leads to the persistent and then normal diffusion, and the latter to the almost normal diffusion. Their effects on the spatial correlation of particle displacement are also studied. [S0031-9007(98)05724-X]

PACS numbers: 52.25.Fi, 63.20.Ry, 66.10.Cb, 82.70.Dd

The Brownian motion of particles in a complex fluctuating background is a historical problem [1]. In particular, the anomalous diffusion driven by mechanisms other than ordinary diffusion has been shown to play a fundamental role in the dynamics of a wide class of complex systems such as porous medium [1], colloidal suspensions [2,3], rotating and turbulent flows [1,4,5], surface waves [6], etc. The unusual topological features and spatiotemporal correlations can make the mean square displacement $\langle(\Delta R)^2\rangle \propto t^H$, with H deviating from 1 which is the exponent for the normal diffusion [1].

In a strongly coupled many body Coulomb system around melting or in the liquid state, each particle couples with a background which intrinsically has a large number of degrees of freedom but is not completely disordered. The strong mutual interaction can constrain particle motion or allow the collective excitations which enhances particle diffusion. For example, for the system with charged colloids suspended in liquid, the cage effect of the surrounding colloids and the rearrangement of cages in the freezing state lead to the transition from the small amplitude normal diffusion induced by the dense background liquid to the antipersistent diffusion with $H < 1$, and then back to the dressed normal diffusion with increasing time [2].

Recently, the formation of crystals and liquids with micrometer size fine dust particles suspended in glow discharges were demonstrated in several laboratories [7–11]. Basically, the dust particles can be easily charged to 10^4 electrons in the gaseous plasma background and form a strongly coupled Coulomb system. The coupling between the dust particle motion and the surrounding lattice is through mainly the direct Coulomb interaction. Under the much lower molecular impact rate from the low pressure background, the hydrodynamic complication and overdamped motion in the colloidal liquid suspensions can be avoided [2,3]. Different motions and excitations are thereby expected. The long relaxation time also allows the direct optical tracking for individual particle motion. In our previous experiments [10,11], different self-excited rotational domains and associated defect motions for a hexagonal cylinder structure around melting were observed. The static translational and orientational orders were also investigated by measuring the static pair correlation functions for particle position and orientation in other systems [12,13]. However, the excitation dynamics and the relations with diffusion at different time scales in the melting and liquid phases are poorly understood. Moreover, unlike the vertical migration in the other system [12,13], the particles in our system move only on the horizontal plane. It makes a good quasi-2D system and allows long term particle tracking without losing particles.

In this work, for the first time, we study the diffusion properties of the melting and liquid states in this system. Starting from the antipersistent motion with small displacement in the initial caged regime, we further explore the dynamical behavior of thermally excited rotational domains and their impact on the spatiotemporal behavior of particle transport over three decades of time scale. The melting state is relatively hard and brittle. The random phase excitation and reorganization of the rotational domains follow the stick-slip type rule, and lead to the persistent diffusion ($H = 1.31$) and the normal diffusion ($H = 1$) in the intermediate and long time regimes, respectively. The liquid state is much softer. The random phase rotational excitation still provides spatial coupling but is no longer stick-slip type. It switches the diffusion directly from the caged antipersistent regime to the almost uncorrelated regime ($H = 1.07$) with increasing time.

The experiment is conducted in a cylindrical symmetric rf dusty plasma system as described elsewhere [7]. Through the chemical reaction between oxygen and silane gas mixtures, micrometer sized fine SiO_2 particles are formed, negatively charged, suspended, and trapped in an annular groove (with 1.3 cm width and 6 cm diameter) of a rf(14 MHz) low pressure (250 mTorr) Ar discharge system ($n_e \approx 10^9$ cm^{-3}). Increasing rf power can change the system from solid to liquid without other external perturbation. The strong vertical ion flow, the slightly polydispersive particle size distribution, and the long vertical chains might be the causes preventing vertical migration. The system is uniform over more than 25 lattice constants

both along the vertical and radial directions. The particle motion on a plane in the center part of the groove is monitored by a digital video recording system (with 30 Hz frame rate) through an optical microscope.

Figure 1 shows the single particle mean square displacement [SMSD, $\langle(\Delta R)^2\rangle$]. Each SMSD point is obtained by averaging over particle displacements from 30 sets of picture frames, with 240 sequential frames and different starting times for each set, and about 120 particles for each frame. Basically, for the state around melting, the diffusion can be roughly divided into three different regimes with $H < 1, = 1.31 \pm 0.08$, and $= 1 \pm 0.06$, respectively, at different time (length) scales. This behavior is obviously different from the diffusion property in the strongly coupled colloidal suspensions in liquids. It can be easily understood through Fig. 2, which shows the typical displacements along the x axis (ΔX) of dust particles initially sitting at the sites indicated in Fig. 2(b) with 0.3 s sampling rate. The typical short time behavior with $\frac{1}{30}$ s sampling rate is shown in Fig. 2(a). The antipersistent motion in regime I with a high rate of reversing the moving direction within a few sampling steps, and the similar displacements with a slight phase difference for adjacent particles after low pass filtering the signals (the dashed lines) are due to the initial cage effect from the surrounding particles. Regime I ends when SMSD approaches $(0.2a)^2$ ($a = 0.27$ mm: it is the mean nearest neighbor particle separation measured from the first peak of the pair correlation function), which is about the distance for the Linderman criteria.

The self-organized vortex type motion plays the dominant role for the particle transport in regime II. From our previous study, we learn that the rotational domain has higher velocity for the particles closer to the domain boundary [10,11]. The relative domain motion can cause strong shear for particles separated one a apart across domain boundaries. From Fig. 2, we can further understand the time scale for domain motion and the spatial correlation between particles. The sudden jumps at t_1, t_3, t_6, etc., are due to the sudden onset of domain slipping. At t_1, particles A, B, and C move toward the right, and D and E move toward the left. Namely, particles A-B-C and D-E belong to two different domains for the excitation at t_1, which induces strong shear. The displacement of particle F (the one above D and E) has smoother transition than

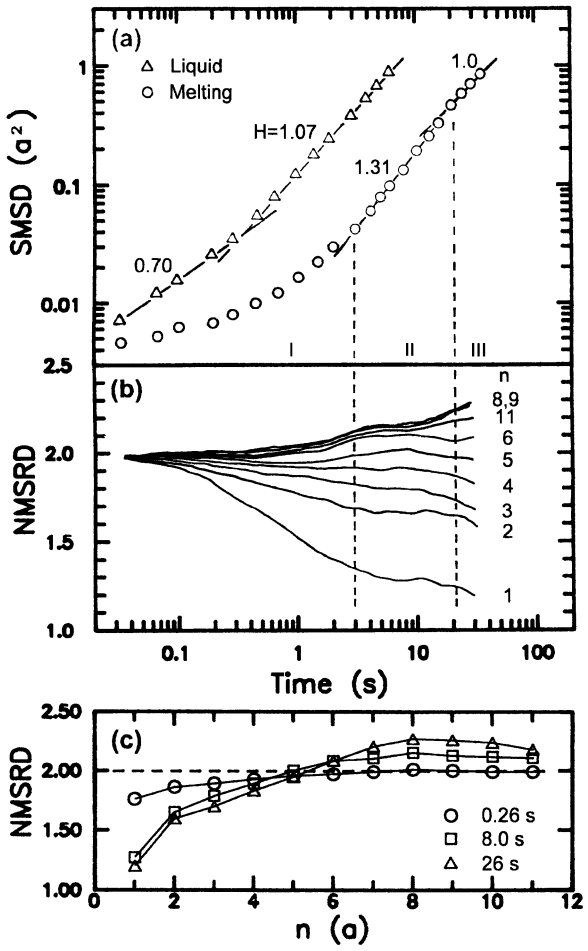

FIG. 1. (a) SMSD versus time for the melting and liquid states. (b) NMSRD versus time for particle pairs with different separations na of the melting state. (c) NMSRD versus n at three different times for the melting state.

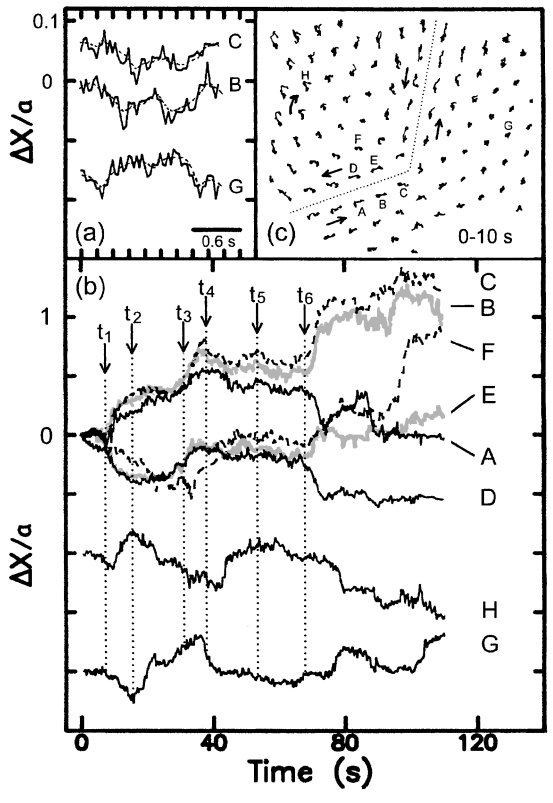

FIG. 2. (a),(b) The typical short and long time particle displacements along the x axis in the melting state with 0.3 and $\frac{1}{30}$ s frame rates, respectively. Their corresponding positions can be found in (c) which shows the 2D trajectories over 10 s.

those of D and E, because it is closer to the center of the upper rotational domain. The high speed collective domain rotation lasts only approximately a few seconds, and ceases when the relative displacement across the boundary between the two domains reaches about 1 lattice constant. After the rotation (e.g., after t_2), the particles have only small amplitude collective fluctuations. At t_3, there is another jump due to the onset of the second rotational motion. This time, particles A to E all move along the same direction. It means that the domain boundary excited at t_1 disappears after t_2, and they all belong to the same domain before the excitation at t_6. The excitation at t_6 separates particles A-D and B-C-E-F into two different domains.

The above observation manifests that the domain rotation and reorganization around melting follows the stick-slip rule similar to the earthquake. The distortion of lattice in the sticking period builds up strain energy which is suddenly released through excitation of the rotational domain by cracking at the sites where the lattice distortions are beyond certain threshold. Cracking also limits domain size and causes strong shears. Therefore, the relative deviation of particle displacements before the sudden slip in Fig. 2(b) (e.g., before t_6) can be treated as a precursor for opposite motions crossing the new domain boundary during slipping. The slipping lasts for a few seconds. Note that it never travels more than $1a$. It stops when the particles across the domain boundary realign along the lattice line. The old domain boundary (the crack) disappears. The particles around that region enter the new sticking period. The kinetic energy of slipping can be dissipated through phonons to the surrounding lattice regions to induce their rocking (if the energy is not enough to break bonds) or further slipping, or partially to the background neutral gas (the dust-neutral relaxation time is about a few seconds). For example, particles G and H start to have large displacements slightly after t_1, but they rock back after t_2. The finite particle inertia causes the phase lag for particle displacements along the traveling direction. Particles A to F also oscillate between t_4 and t_6. For a time scale longer than the two successive slips or rockings, the single particle motion loses memory, and the diffusion switches from the persistent regime II with $H > 1$ to the uncorrelated regime III with $H = 1$.

We further study the spatial correlation of motion by measuring the mean square relative displacement (MSRD) between two particles initially separated with (na). Figure 1(b) plots the normalized MSRD(NMSRD) with respect to SMSD. $\mathrm{MSRD} = \langle(\Delta R_i - \Delta R_j)^2\rangle = 2\langle(\Delta R_i)^2\rangle - 2\langle\Delta R_i \Delta R_j\rangle = 2\mathrm{SMSD} - 2\langle\Delta R_i \Delta R_j\rangle$, and $\mathrm{NMSRD} = \mathrm{MSRD}/\mathrm{SMSD} = 2 - 2\langle\Delta R_i \Delta R_j\rangle/\langle(\Delta R_i)^2\rangle$, where $\Delta R_i \Delta R_j$ is the vector product of the displacements of two particles i and j initially separated with na. The errors of NMSRDs are about 0.05. The particle pair motions are correlated (anticorrelated) if NMSRD $< (>)$ 2.

At the beginning, NRMSD ≈ 2. The high frequency and small amplitude pair motions are uncorrelated. The gradually increasing displacement builds up spatial correlation and makes the deviation of NRMSD from 2 increase with time. As n increases, NMSRD asymptotically reaches 2 from below in the first half of regime I [Fig. 1(c)]. It indicates that under small displacement, only the near neighbor particle motions are correlated due to a cage effect through direct Coulomb interaction. The far pair shows quite unlike short-time motions [Fig. 2(a)].

In the transition region between I and II, the correlation length increases with increasing displacement because lattice distortion can no longer be locally adjusted. The vortex motion becomes important. NMSRD > 2 for $n > 5$ and SMSD $> (0.1a)^2$ indicates the anticorrelated long range pair motion. If na is larger than the mean radius of the domain, the particle pair moving with opposite directions due either to the rotation in the same domain (on the opposite sites with respect to the rotation center) or crossing the domain boundary has a main contribution on the anticorrelated motion. NMSRD > 2 for $n > 5$ and starts to turn back to 2 for $n > 9$ in regimes II and III. Namely, the mean domain radius is about a few a, and the spread of domain size makes the correlation decrease for separation beyond this scale. Comparing the displacements of particles A, G, and H in Fig. 2 evidences the weakly anticorrelated motion at a long distance. In regime II, NMSRD levels as time increases. It implies that H is similar for MSRD and SMSD, because they all originate from collective domain motion. The decreasing (increasing) NMSRD with time in regime III for $n < (>) 5a$ indicates that the pair correlation is not destroyed by the two successive random phase slips. Figure 2 shows that the relative mean displacement for adjacent particles increases less drastically in time than the single particle displacement caused by domain rotation.

In the liquid state at higher rf power, the system is less brittle than the melting state. The stronger random motion due to the weaker Coulomb coupling makes H larger ($H = 0.70 \pm 0.08$) in the initial caged regime. Under a larger thermal energy fluctuation, no typical time scale is required to overcome the energy barrier for rotation. The long range rotational motion does not follow the stick-slip rule [see the typical motions in Fig. 3(a)]. It directly causes crossing from the antipersistent caged regime I to regime II with $H = 1.07 \pm 0.06$, which is quite close to the normal diffusion. Similar to the melting state, regime I also ends around SMSD $= (0.2a)^2$. Note that, unlike in the other dusty plasma system [12], both the melting and liquid states show no vertical migrations. The large scale motions on the horizontal plane must be rotational due to the low compressibility. Although the liquid has much shorter translation and orientation correlation lengths for particle positions, the rotational motion still provides the spatial correlation for particle displacement similar to that of the harder melting state with only a slightly shorter length scale, but 1 order of

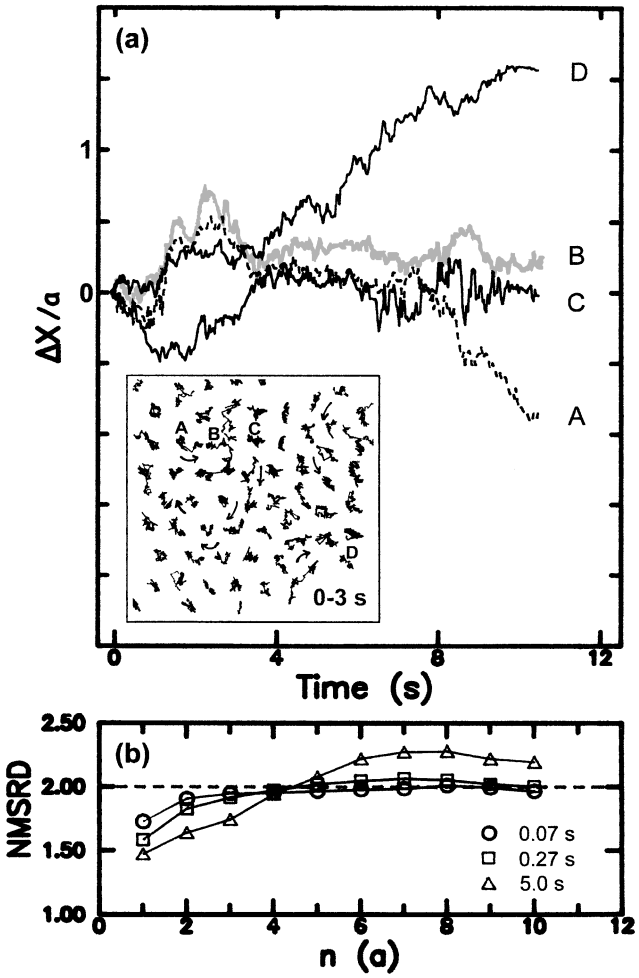

FIG. 3. (a) The typical particle displacements along the x axis for the liquid state. Their corresponding positions can be found in the inset which shows the 2D trajectories. (b) NMSRD versus n at different times for the liquid state.

magnitude faster time scale. Figure 3 shows that NMSRD asymptotically reaches zero as n increases in the short time regime and crosses 2 around $n = 4$ for rotational motion in the long time regime.

In conclusion, the vortex dynamics and the diffusion properties are studied in a strongly coupled quasi-2D system. Initially, the cage effect induced by the near neighbors causes antipersistent diffusion. The spatial correlation of displacement gradually builds up as time (or displacement) increases. For SMSD $> (0.2a)^2$, long range collective motion dominates the particle transport. For the brittle melting state, the stick-slip type domain rocking and rotation with varying domain sizes and strong shears (cracking) around boundaries are responsible for the persistent diffusion. The single particle motion is uncorrelated in time for time longer than the dephasing time of the rotational excitation, and SMSD $> (0.7a)^2$. The NMSRD measurement also shows that the mean domain size is about a few a. In the liquid state, the system is softer and with larger H in the initial antipersistent regime. The vortex motion with a slightly shorter effective diameter is still responsible for collective transport, regardless of the much shorter translation and orientation correlation for positions comparing to the melting state. The non-stick-slip type rotational excitation and relaxation directly make H close to 1 for SMSD $> (0.2a)^2$.

This work is supported by the National Science Council of the Republic of China under Contract No. NSC-86-0212-M008-006.

[1] For example, J. Feder, in *Fractals* (Plenum Press, New York, 1988), Chap. 9; J. Klafter, M. F. Shlesinger, and G. Zumofen, Phys. Today **49**, No. 2, 33 (1995).
[2] H. Lowen, T. Palberg, and R. Simon, Phys. Rev. Lett. **70**, 1557 (1993); A. V. Indrani and S. Ramaswamy, Phys. Rev. Lett. **73**, 360 (1994).
[3] A. J. C. Ladd, H. Gang, J. X. Zhu, and D. A. Weitz, Phys. Rev. Lett. **74**, 318 (1995).
[4] T. H. Solomon, E. R. Weeks, and H. L. Swinney, Phys. Rev. Lett. **71**, 3975 (1993).
[5] T. Bohr and A. Pikovsky, Phys. Rev. Lett. **70**, 2892 (1993).
[6] E. Schroder, J. S. Andersen, M. T. Levinsen, P. Alstrom, and W. I. Goldburg, Phys. Rev. Lett. **76**, 4717 (1996).
[7] J. H. Chu and Lin I, Physica (Amsterdam) **205A**, 183 (1994); J. H. Chu and Lin I, Phys. Rev. Lett. **72**, 4009 (1994).
[8] Y. Hayashi and K. Tachibana, Jpn. J. Appl. Phys. **33**, 804 (1994).
[9] H. Thomas, G. E. Morfill, V. Demmel, J. Goree, B. Feuerbacher, and D. Mohmann, Phys. Rev. Lett. **73**, 652 (1994).
[10] C. H. Chiang and Lin I, Phys. Rev. Lett. **77**, 647 (1996).
[11] Lin I, W. T. Juan, and C. H. Chiang, Science **272**, 1626 (1996).
[12] H. M. Thomas and G. E. Morfill, Nature (London) **379**, 806 (1996).
[13] A. Melzer, A. Homann, and A. Piel, Phys. Rev. E **53**, 2757 (1996).